Materials Science and Engineering B 175 (2010) 41–43

Contents lists available at ScienceDirect

Materials Science and Engineering B

journal homepage: www.elsevier.com/locate/mseb

Characterization of $Mg_{0.20}Zn_{0.80}O$ metal–semiconductor–metal photodetectors

Dayong Jiang[a], Xiyan Zhang[a,*], Quansheng Liu[a], Zhaohui Bai[a], Liping Lu[a], Xiaochun Wang[a], Xiaoyun Mi[a], Nengli Wang[a], Dezhen Shen[b]

[a] School of Materials Science and Engineering, Changchun University of Science and Technology, Changchun 130022, China
[b] Key Laboratory of Excited State Processes, Changchun Institute of Optics, Fine Mechanics and Physics, Chinese Academy of Sciences, Changchun 130033, China

ARTICLE INFO

Article history:
Received 18 March 2010
Received in revised form 28 May 2010
Accepted 9 June 2010

Keywords:
$Mg_xZn_{1-x}O$
Photodetector
MSM
Responsivity
Dark current

ABSTRACT

$Mg_{0.20}Zn_{0.80}O$ films have been prepared on quartz substrates by using radio frequency (RF) magnetron sputtering, and metal–semiconductor–metal (MSM) structured photodetectors have been fabricated on the $Mg_{0.20}Zn_{0.80}O$ films employing interdigital Au as metal contacts. We have investigated the effects of electrode spacings on the properties of $Mg_{0.20}Zn_{0.80}O$ MSM photodetectors. It was shown that both of dark currents and responsivities of the devices will decrease with the increasing electrode spacing at the same bias. It was thought that the resistance and the depletion region between the electrodes play important roles in the devices, and the physical mechanism can be explained by a straightforward qualitative model.

Published by Elsevier B.V.

1. Introduction

$Mg_xZn_{1-x}O$ has been subjects of intense scientific research as wide band gap optoelectronic materials. Its excellent material properties are promising for ultraviolet (UV) photon detectors [1–4]. Compared with GaN based material system, it has been reported that the saturation velocity of $Mg_xZn_{1-x}O$ is higher, and it has also been found that $Mg_xZn_{1-x}O$ is less susceptible to irradiation effects [5]. Furthermore, $Mg_xZn_{1-x}O$ has lower charged dislocation scattering and interface scattering. Thus, $Mg_xZn_{1-x}O$ based photodetectors are extremely useful for UV light sensing. Recently, there have been lots of reports on good quality $Mg_xZn_{1-x}O$ films fabricated by the well-known techniques such as metalorganic chemical vapor deposition (MOCVD) [6,7], molecular beam epitaxy (MBE) [8,9], RF magnetron sputtering [10,11], and pulsed laser deposition (PLD) [12,13]. Among these techniques, the operation of RF magnetron sputtering is simple and has lower cost.

Due to the challenges of reliable p-type doping of $Mg_xZn_{1-x}O$ that hinder the realization of p–n junction-based devices, the MSM structure has been preferentially considered for the photodetector applications [14,15]. It is well known that MSM photodetectors have several advantages compared with traditional p–n photodiodes. Firstly, they have a planar structure, which is compatible with most electronic devices, making them ideal for optoelectronic integrated circuit (OEIC) applications. Secondly, because of their geometry, they have a lower capacitance for the same active area resulting in a lower (RC) time delay. Thirdly, the process for fabricating these devices is very simple and compatible with regular IC processes. All of these properties make MSM photodetectors attractive for the high performance photodetection. Furthermore, the electrode spacing will affect the properties of MSM photodetectors obviously, which will result in different resistances, active receiving areas, and capacitances. Unfortunately, there is no report about the role of the electrode spacing. In this work, we report the growth of $Mg_{0.20}Zn_{0.80}O$ thin films and the fabrication of Schottky type $Mg_{0.20}Zn_{0.80}O$ MSM photodetectors. The effects of electrode spacings on the properties of $Mg_{0.20}Zn_{0.80}O$ MSM photodetectors will be discussed.

2. Experiments

$Mg_xZn_{1-x}O$ thin films were grown on quartz substrates by using RF frequency magnetron sputtering technique. A $Mg_{0.1}Zn_{0.9}O$ target was prepared by sintering the mixture of 99.99% MgO and ZnO powders at 1273 K for 10 h in air ambient. Before deposition, the quartz substrates were cleaned in an ultrasonic bath with acetone, ethanol, and de-ionized water at room temperature. The growth chamber was evacuated to a base pressure of 5×10^{-4} Pa, and then filled to 1.0 Pa with mixed gases of 99.99% pure Ar and O_2, which were introduced into the sputtering chamber through a set of mass flow controllers with the rates of 60 and 20 SCCM (standard cubic centimeter per minute), respectively. The substrate temperature was controlled at about 673 K. The rate of deposition is adjusted so as to have a film thickness of nearly 400 nm during the film growth. In order to improve the crystal quality, the sample was annealed at 973 K for 30 min in vacuum. The MSM structure with

* Corresponding author. Tel.: +86 431 85583016; fax: +86 431 85583015.
E-mail address: xiyzhang@126.com (X. Zhang).

0921-5107/$ – see front matter. Published by Elsevier B.V.
doi:10.1016/j.mseb.2010.06.017

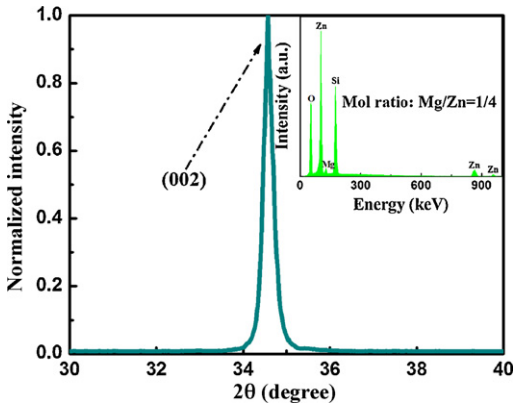

Fig. 1. XRD spectra of the $Mg_xZn_{1-x}O$ thin film prepared on the quartz substrate by RF magnetron sputtering technique. The inset shows the EDS data for the $Mg_xZn_{1-x}O$ thin film.

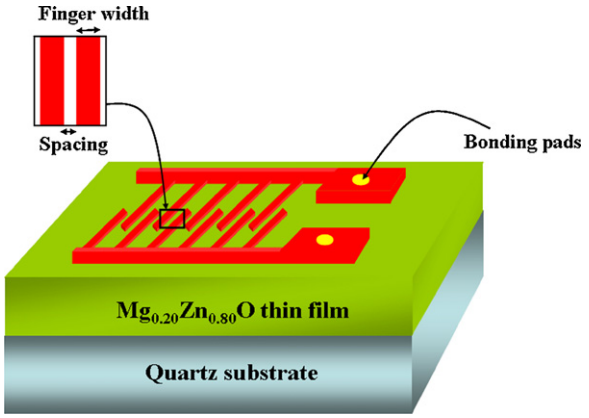

Fig. 3. Schematic illustration of the MSM photodetector showing interdigitated electrodes.

interdigitated configuration on the $Mg_xZn_{1-x}O$ thin film was obtained by lithography and wet etching. It consists of 12 fingers at each Au electrode, which are 5 μm width, and 500 μm long. The spacings of three electrodes are 2, 5, and 10 μm, respectively.

The crystal quality of $Mg_xZn_{1-x}O$ thin films was charactered by an X-ray diffraction (XRD) with Cu Kα (0.154 nm) line as the radiation source. Energy-dispersive X-ray spectroscopy (EDS) (GENESIS 2000 XMS 60S) was used to determine the composition of the films. The transmission and absorption spectra were recorded using a Shimadzu UV-3101PC scanning spectrophotometer. For the characterization of $Mg_xZn_{1-x}O$ MSM photodetectors, a 150 W Xe lamp was used as the excitation source. The spectrum response was measured by a lock-in amplifier. The typical current–voltage (*I–V*) characteristics of the photodetectors were measured by a semiconductor analyzer (Keithley 4200).

3. Results and discussion

The structural property of the $Mg_xZn_{1-x}O$ thin film assessed by XRD and the diffraction pattern of the film is shown in Fig. 1. Only one peak located at 34.6° can be observed for the sample, and this peak can be attributed to the diffraction from (0 0 2) facet of hexagonal $Mg_xZn_{1-x}O$ alloys (JCPDS Card no. 80-0075). The absence of the characteristic peaks of cubic structure indicates that the film has preferred (0 0 2) orientation without phase separation. In order to better understand the Mg composition in the $Mg_xZn_{1-x}O$ thin film, EDS measurement for the film was carried out. The inset of Fig. 1 shows the EDS spectra of $Mg_xZn_{1-x}O$ thin film on quartz substrate, indication the Mg composition about 20%.

Fig. 2 shows the transmission and absorption spectra of the annealing film. The substrate contribution is excluded. There was a steep absorption edge at 320 nm, indicating that there may be few defects in the film. The transmittance in visible region was more than 70%, and such high transmission was helpful to enhance the ultraviolet responsivity.

Dark current is important to the performance of the photodetector since high dark current will introduce noise to the system and make the minimum detectable power higher. Fig. 3 shows the schematic illustration of the interdigitated contacts. *I–V* characteristics of the fabricated $Mg_{0.20}Zn_{0.80}O$ MSM photodetectors were carried out in Fig. 4. All devices exhibited low dark current due to high material resistivity and the rectifying nature of the contacts. As shown in Fig. 4 for $Mg_{0.20}Zn_{0.80}O$ MSM photodetectors, the dark currents were 7.2, 2.1, and 0.4 nA under 3 V bias, which were corresponding to the spacings of 2, 5, 10 μm, respectively. Furthermore, it was clearly shown that the dark current decreased with the increasing spacing. As an important parameter, the spacing will affect the dark current, and the physical mechanism will be discussed in below.

Fig. 5 shows measured spectral response of the fabricated $Mg_{0.20}Zn_{0.80}O$ MSM photodetectors with different spacings. The applied bias voltage was 3 V for each spacing. As shown in Fig. 5, it was found that the responsivities were also different with the spacings in the wavelength region from 300 to 500 nm. The peak responsivity increased with the decreasing spacing and it reached a maximum responsivity of 0.8 A/W with the spacing of 2 μm. Furthermore, the inset of Fig. 5 shows the peak responsivity as a function of bias voltage with the spacing of 2 μm. A nonlinear relationship was obtained, indicating the sweep-out effect up happens at up to 10 V bias.

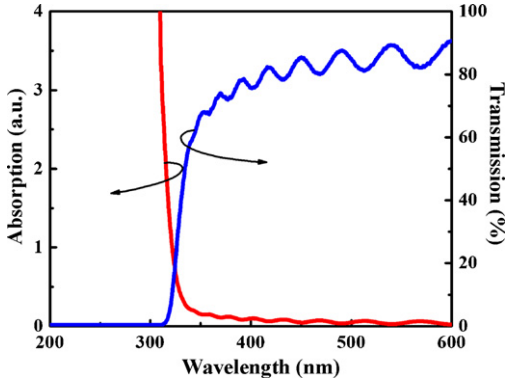

Fig. 2. Transmission and absorption spectra of the $Mg_{0.20}Zn_{0.80}O$ thin film.

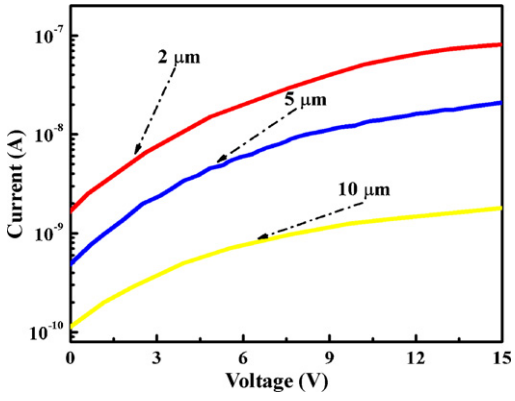

Fig. 4. *I–V* characteristics of the fabricated $Mg_{0.20}Zn_{0.80}O$ MSM photodetectors with different spacings.

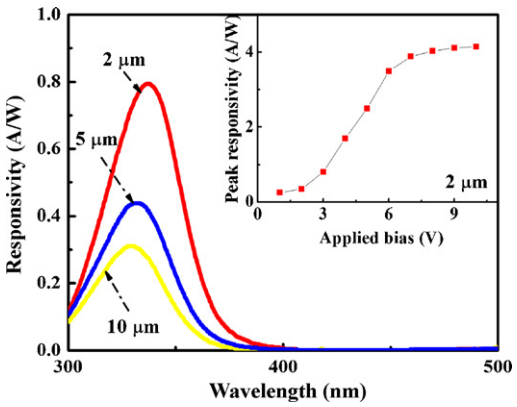

Fig. 5. Spectral response of $Mg_{0.20}Zn_{0.80}O$ MSM photodetectors with different spacings. The inset shows the peak responsivity as a function of bias voltage with the spacing of 2 μm.

Comparing the parameters for these devices, the differences are attributed to the electric fields, which are due to different spacings. It is necessary to make known the distribution of the electric fields, in which the depletion width is the most important parameter. It is known that the MSM structure is basically two Schottky barriers connected back to back. As the applied voltage increases, the sum of the two depletion widths will also increase. Eventually at the reach-through voltage, V_{RT}, the two depletion regions touch each other and the sum equals exactly to the spacing. For a matter reference, we change the spacings with a lower bias voltage of 3 V. The depletion width can be expressed as [16]:

$$W = \sqrt{\frac{2k\varepsilon_0(\psi_0 + V)}{qN_d}}$$

Here k is relative dielectric constant, ε_0 is absolute dielectric constant, ψ_0 is built-in potential, V is the bias voltage, q is electron charge, and N_d is the donor concentration $\sim 10^{16}$ cm^{-3}. We suppose that the whole bias voltage acted on the reverse biased junction, the depletion width was carried out at about 0.6 μm. Therefore, the actual sum of two depletion widths will be less than 2 μm obviously, indicating that the bias could not achieve V_{RT}. Then we can establish the model of the electric field, and the potential profile of the 1-dimensional (D) MSM structure, as shown in Fig. 6.

Based on the model, the physical mechanism of the formation different parameters for all devices can be explained. (1) The explanation for the dark currents: we confirm that the length L will be widened with the increasing spacing. This results in the increasing resistance, which is the main reason for the lower dark current. For the spacing of 10 μm, the dark current was the lowest of 0.4 nA. (2) The explanation for the responsivities: it is noted that the responsivity is proportional to the electric field between the electrodes. The active receiving area for the MSM photodetectors was the depletion region. When the bias voltage was applied, any free carries including the photogenerated carriers exist in this region will be swept out by the high electric field and drift at their terminal velocities to the metal electrodes. The sum of the two depletion widths will expand with the increasing applied voltage. As mentioned above, when the applied voltage was a constant, the resistance will be larger with the increasing spacing. So the voltage on the resistance of the length L will be enhanced, implying that the voltage acting on the depletion region will decrease. We deduce that the depletion region will be shorter at the same time, which is equal to the reducing of the active receiving area. Then, the amount of photogenerated carriers will also decrease. Obviously, the varied trend of the responsivity was contrary to the increasing spacing.

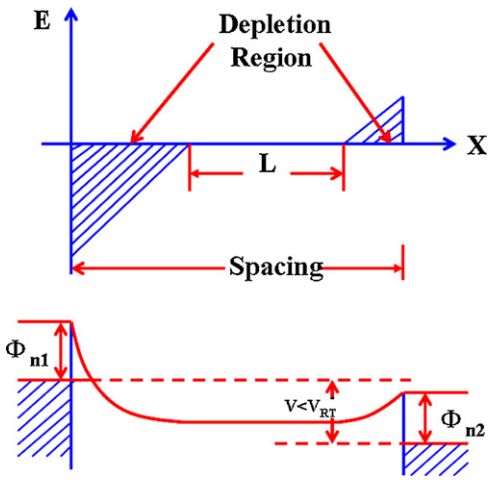

Fig. 6. Model of the electric field, and the potential profile of 1D MSM structure before achieving V_{RT}.

4. Conclusions

$Mg_{0.20}Zn_{0.80}O$ MSM photodetectors with different spacings were fabricated and characterized. It was found that the dark current decreased with the increasing spacing, which was attributed to the enhanced resistance between the electrodes. It should be noted that all dark currents were below 10 nA at 3 V. However, the applied bias voltage, 3 V, could not achieve V_{RT} for the shortest spacing, it was also showed that the highest responsivity of 0.8 A/W corresponding to the shortest spacing, which was due to the widen depletion region. The research indicates that we should enhance the Schottky barrier and adopt short spacings to fabricate MSM photodetectors. We believe that these results represent a significant step toward achieving practical solid state UV photodetectors based on $Mg_xZn_{1-x}O$ material system.

Acknowledgement

This work is supported by the National Natural Science Foundation of China under grant no. 50772016.

References

[1] X.L. Du, Z.X. Mei, Z.L. Liu, Y. Guo, T.C. Zhang, Y.N. Hou, Z. Zhang, Q.K. Xue, A.Y. Kuznetsov, Adv. Mater. 21 (2009) 4625.
[2] W. Yang, R.D. Vispute, S. Choopun, R.P. Sharma, T. Venkatesan, H. Shen, Appl. Phys. Lett. 78 (2001) 2787.
[3] I. Takeuchi, W. Yang, K.S. Chang, M.A. Aronova, T. Venkatesan, R.D. Vispute, J. Appl. Phys. 94 (2003) 7336.
[4] Y.F.B. Yao, R. Deng, B.H. Li, J.Y. Zhang, Y.M. Zhao, D.Y. Jiang, Z.Z. Zhang, C.X. Shan, D.Z. Shen, X.W. Fan, Y.M. Lu, J. Phys. D: Appl. Phys. 42 (2009) 105102.
[5] L. Pintilie, I. Pintilie, Mater. Sci. Eng. B 80 (2001) 388.
[6] T. Gruber, C. kirchner, R. Kling, F. Reuss, A. Waag, Appl. Phys. Lett. 84 (2004) 5359.
[7] W. Liu, S.L. Gu, S.M. Zhu, J.D. Ye, F. Qin, S.M. Liu, X. Zhou, L.Q. Hu, R. Zhang, Y. Shi, Y.D. Zheng, J. Cryst. Growth 227 (2005) 416.
[8] Z.P. Wei, Y.M. Lu, D.Z. Shen, C.X. Wu, Z.Z. Zhang, D.X. Zhao, J.Y. Zhang, X.W. Fan, J. Lumin. 119 (2006) 551.
[9] K. Ogata, K. Koike, T. Tanite, T. Komuro, F. Yan, S. Sasa, M. Inoue, M. Yano, J. Cryst. Growth 251 (2003) 623.
[10] X.L. Xu, L. Lu, Y. Wang, C.S. Shi, J. Phys.: Condens. Matter 18 (2006) 1189.
[11] S. Kumar, V. Gupte, K. Sreenivas, J. Phys.: Condens. Matter 18 (2006) 3343.
[12] A.K. Sharma, J. Narayan, J.F. Muth, C.W. Teng, C. Jin, A. Kvit, R.M. Kolbas, O.W. Holland, Appl. Phys. Lett. 75 (1999) 3327.
[13] S. Choopun, R.D. Vispute, W. Yang, R.P. Sharma, T. Venkatesan, H. Shen, Appl. Phys. Lett. 80 (2002) 1529.
[14] S.J. Young, L.W. Ji, R.W. Chuang, S.J. Chang, X.L. Du, Semicond. Sci. Technol. 21 (2006) 1507.
[15] Q.A. Xu, J.W. Zhang, K.R. Ju, X.D. Yang, X. Hou, J. Cryst. Growth 289 (2006) 44.
[16] U.K. Mishra, J. Singh, Semiconductor Device Physics and Design, Springer, Netherlands, 2007.